Establishment of smooth muscle and cartilage juxtaposition in the developing mouse upper airways

Elizabeth A. Hines, Mary-Kayt N. Jones, Jamie M. Verheyden, Julie F. Harvey, and Xin Sun[1]

Laboratory of Genetics, University of Wisconsin, Madison, WI 53706

Edited by Janet Rossant, Hospital for Sick Children, University of Toronto, Toronto, ON, Canada, and approved October 21, 2013 (received for review July 12, 2013)

In the trachea and bronchi of the mouse, airway smooth muscle (SM) and cartilage are localized to complementary domains surrounding the airway epithelium. Proper juxtaposition of these tissues ensures a balance of elasticity and rigidity that is critical for effective air passage. It is unknown how this tissue complementation is established during development. Here we dissect the developmental relationship between these tissues by genetically disrupting SM formation (through *Srf* inactivation) or cartilage formation (through *Sox9* inactivation) and assessing the impact on the remaining lineage. We found that, in the trachea and main bronchi, loss of SM or cartilage resulted in an increase in cell number of the remaining lineage, namely the cartilage or SM, respectively. However, only in the main bronchi, but not in the trachea, did the loss of SM or cartilage lead to a circumferential expansion of the remaining cartilage or SM domain, respectively. In addition to SM defects, cartilage-deficient tracheas displayed epithelial phenotypes, including decreased basal cell number, precocious club cell differentiation, and increased secretoglobin expression. These findings together delineate the mechanisms through which a cell-autonomous disruption of one structural tissue can have widespread consequences on upper airway function.

airway development | tracheomalacia

The trachea and the main bronchi, here collectively termed the upper airways, are essential conduits of air before and after gas exchange (1, 2). Normal upper airways offer the correct balance of elasticity and rigidity, which together maintain air pressure and prevent airway collapse. The elasticity is primarily provided by smooth muscle (SM) and the rigidity by cartilage. The balance is achieved via a precise juxtaposition of these tissues that together encircle and support the endoderm-derived upper airway epithelium. Clinical evidence suggests that malformation of the SM or cartilage leads to respiratory deficiencies. For example, patients with tracheomalacia and bronchomalacia exhibit airway collapse upon exhalation as a result of softened and disorganized cartilage (3). This collapse causes breathing difficulties that contribute to sleep apnea, respiratory infections, and possibly sudden infant death (4). Despite the importance of a proper SM and cartilage balance, how it is achieved during development is not understood.

In mouse upper airways, SM is localized to the dorsal side of the trachea and the medial (inner) sides of the main bronchi. The lower conducting airways lack cartilage and instead SM surrounds the circumference of the epithelial tube. Data suggest that airway SM develops from fibroblast growth factor 10 (*Fgf10*)-expressing cells found in the distal mesenchyme (5). As the epithelial buds elongate, the *Fgf10*-expressing cells are thought to translocate proximally along the airway and begin to express SM-specific genes, including SM α-actin-2 (*Acta2*, also known as SM actin), one of the earliest markers of SM. Additionally, a recent study has used genetic lineage tracing to demonstrate that cardiac–pulmonary progenitor cells give rise to airway SM (6). In SM outside of the upper airway and lung, it is known that the transcription factors serum response factor (SRF) and MYOCARDIN activate *Acta2* expression (7). In the lung, signals such as sonic hedgehog and WNT2 have been shown to promote SM differentiation (8, 9).

Abutting the SM, airway cartilage is localized to the ventral side of the trachea and the lateral (outer) sides of the main bronchi. Cartilage initiation is marked by mesenchymal expression of SRY-box 9 (*Sox9*), a transcription factor necessary for cartilage development (10). SOX9 acts by promoting *Sox5* and *Sox6* expression, and together these factors induce expression of a key extra-cellular matrix (ECM) molecule, *Col2a1* (11, 12). Multiple signaling genes, including those in the WNT, RA, TGF-β, and FGF pathways, have also been implicated in upper airway cartilage development (13–16). Despite these findings on the genetic control of airway SM and cartilage formation, little is known regarding how their development is coordinated.

The epithelium subjacent to the SM and cartilage is composed of a number of cell types with specialized functions. For example, ciliated cells are responsible for foreign particle clearance, club (formerly Clara) cells help to maintain a moist airway, and basal cells can serve as progenitors in the event of airway damage (1, 2, 17). Defects in the number, function, and/or distribution of these epithelial cell types are often central to the pathophysiology of lung diseases. For example, individuals with immotile ciliary syndrome have decreased ciliated cell number and/or function that causes decreased mucociliary clearance and increased respiratory infection (18). In individuals with asthma, chronic obstructive pulmonary disorder, or cystic fibrosis, goblet cell metaplasia contributes to improper mucous accumulation (19).

Airway epithelial cell types initiate their differentiation after the establishment of the SM and cartilage pattern. For example, ciliated cells begin to express *Foxj1* at embryonic day (E) 15.5 and club cells begin to express secretoglobin family 1A member 1 (*Scgb1a1*) at E16.5 (17). Basal cells, marked by transformation related protein 63 (*p63*) expression, are located in the basement layer of the pseudostratified tracheal epithelium (20). A subset of

Significance

A balance of airway rigidity and elasticity is critical for uninterrupted airflow to and from the lungs. In the trachea and bronchi, this balance is achieved by the precise juxtaposition of smooth muscle (SM) and cartilage that together encircle the airway. We investigate how this juxtaposition is established during embryogenesis by using mouse mutants that lack either SM or cartilage in the developing lung. We demonstrate the nature of the antagonism between the nascent SM and cartilage lineages. Our results also reveal a role for cartilage in the proper differentiation of tracheal epithelium. Together these findings elucidate unique mechanisms of how airway SM or cartilage malformation may impact airway function.

Author contributions: E.A.H. and X.S. designed research; E.A.H., M-K.N.J., J.M.V., and J.F.H. performed research; E.A.H. contributed new reagents/analytic tools; E.A.H. and J.M.V. analyzed data; and E.A.H. and X.S. wrote the paper.

The authors declare no conflict of interest.

This article is a PNAS Direct Submission.

[1]To whom correspondence should be addressed. E-mail: xsun@wisc.edu.

This article contains supporting information online at www.pnas.org/lookup/suppl/doi:10.1073/pnas.1313223110/-/DCSupplemental.

these P63$^+$ basal cells further differentiate into keratin-positive (KRT5$^+$ and KRT14$^+$) basal cells, which serve as progenitor cells to repopulate the airway following injury (21–23). Elegant tissue recombination studies have shown that combining tracheal mesenchyme with distal lung epithelium in explant culture led to formation of nonbranched epithelium that contained differentiated ciliated and secretary cells of the trachea (24). This finding suggests that the tracheal mesenchyme provides instructive cues for epithelial cell differentiation. Following SO_2 injury in the adult airway, BrdU-retaining epithelial cells were identified adjacent to the cartilage, suggesting that cartilage may affect the dynamics of airway repair (25). However, during embryonic development, it is unknown if SM and cartilage, being two compartments of the tracheal mesenchyme, exert similar or distinct influences on epithelial differentiation.

The close spatial proximity of SM, cartilage, and the underlying epithelium led us to hypothesize that the development of these tissues is coordinated. To investigate this possibility, we inhibited SM and cartilage formation independently through conditional gene inactivation, and assessed the impact each had on the development of adjacent tissues. Our data delineate the specific nature of the relationships among the upper airway tissue lineages during their development.

Results

Cartilage and SM Develop in Temporal Synchrony and Spatial Complementation. To understand how the juxtaposition of the SM and cartilage is achieved through development, we examined their spatial and temporal relationship by performing expression analysis for the earliest markers of these lineages: *Acta2* for SM and *Sox9* for cartilage. At E10.5, *Acta2* RNA was observed only in the mesenchyme overlying the carina (the point where the trachea splits into the main bronchi), whereas a low-level mesenchymal *Sox9* expression was observed in the length of the trachea and main bronchi (Fig. 1 *A* and *B*). More intense *Sox9* expression was also detected in the distal epithelium, and this epithelial expression continued at later stages. Double immunostaining by using anti-ACTA2 and anti-SOX9 antibodies in transverse sections revealed primarily uncondensed SOX9$^+$ cells that were already restricted to the ventral trachea and lateral main bronchi (Fig. 1 *C* and *D*). ACTA2$^+$ cells were rarely detected, reflecting a delay in the translation of the localized RNA into protein. By E11.5, the *Acta2* RNA domain expanded proximally along the trachea and distally along the main bronchi, whereas *Sox9* mesenchymal expression intensified in the same regions as earlier (Fig. 1 *E* and *F*). In transverse sections, ACTA2$^+$ cells were present along the dorsal trachea and the medial main bronchi whereas SOX9$^+$ cells were condensed along the ventral trachea and lateral main bronchi (Fig. 1*G*, *H*). By E12.5, *Acta2* RNA expression intensified in the extrapulmonary airways and the domain continued to expand distally into the branching regions of the lung (Fig. 1*I*). *Sox9* mesenchymal expression continued to intensify and remained restricted to the unbranched regions of the upper airways (Fig. 1*J*). In immunostained transverse sections, ACTA2$^+$ cells and SOX9$^+$ cells increased in number compared with E11.5, and their spatial complementation continued (Fig. 1 *K* and *L*). This expression analysis revealed that SM and cartilage cells are localized to separate domains from their initiation. The coordinated early development of SM and cartilage establishes a foundation of tissue juxtaposition that will provide the balance of elasticity and rigidity required at birth.

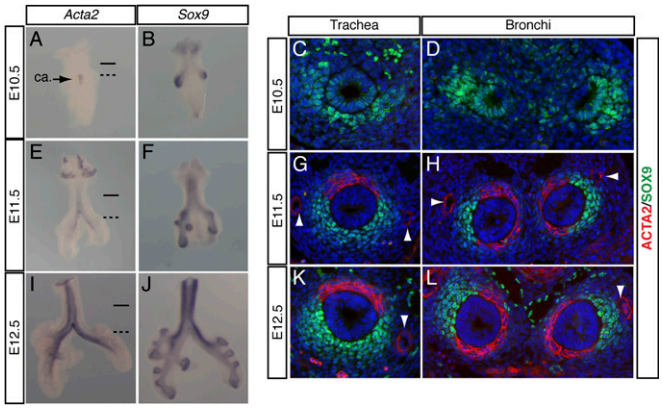

Fig. 1. Temporal and spatial relationship of SM and cartilage in WT embryonic trachea and bronchi. (*A*, *B*, *E*, *F*, *I*, and *J*) RNA in situ hybridization of lungs for *Acta2* or *Sox9* at indicated stages. Solid lines indicate approximate planes of tracheal transverse sections in *C*, *G*, and *K*; dashed lines indicate the approximate planes of bronchial transverse sections in *D*, *H*, and *L*. (*C*, *D*, *G*, *H*, *K*, and *L*) Immunofluorescence staining for ACTA2 (red), SOX9 (green), and nuclei (DAPI; blue) of transverse sections of trachea or main bronchi at indicated stages. White arrowheads indicate the pulmonary artery. ca., carina.

Conditional Deletion of *Srf* Resulted in a Loss of SM and an Increase in Cartilage in the Embryonic Upper Airways. To determine if the normal development of SM is required for the proper patterning of cartilage in the upper airways, we conditionally inactivated a key SM differentiation gene, *Srf*, in the lung using a conditional allele of *Srf* (*Srf^{Fl}*) and forkhead box G1 (*Foxg1*) *-cre*, which is active in the early lung among other tissues (26, 27). *Foxg1-cre*; *Srf $^{Fl/Fl}$* (hereafter *Foxg1cre*;*Srf*) embryos die prenatally at approximately E13.0, possibly because of loss of *Srf* function in tissues such as the heart. Before the stage of lethality, we were able to assess the effect of *Srf* loss in lung development. At E12.5, *Foxg1cre*;*Srf* mutant lungs were smaller compared with control, suggestive of a requirement for *Srf* in promoting lung growth (Fig. 2 *A* and *B*). Strikingly, there was a complete lack of *Acta2* expression in *Foxg1cre*;*Srf* mutants, indicating an absence of airway SM (Fig. 2 *A* and *B*).

To determine if this loss of SM affected cartilage development, the number of SOX9$^+$ cells and the percentage of the airway epithelium circumference in contact with SOX9$^+$ cells (termed cartilage airway coverage) was assessed in the trachea and main bronchi of mutant and control tissues ($n = 3$ samples for each of mutant and control, and $n = 3$ sections per sample). In the trachea, there was a statistically significant increase of SOX9$^+$ cells in the mutant compared with control (33% increase, $P = 0.049$; control, 113 ± 9.9; *Foxg1cre*;*Srf*, 150.5 ± 7.6; Fig. 2 *C*, *D*, and *G*). Interestingly, no significant difference was observed in the tracheal cartilage airway coverage ($P = 0.332$; control, 68 ± 2.5%; *Foxg1cre*;*Srf*, 73% ± 2.8; Fig. 2 *C*, *D*, and *H*). In the main bronchi, there was an increase in SOX9$^+$ cells trending toward significance (76% increase, $P = 0.080$; control, 90.3 ± 5.2; *Foxg1cre*;*Srf*, 159 ± 16.1; Fig. 2 *E*, *F*, and *I*). However, unlike in the trachea, there was a significant increase in cartilage airway coverage of the main bronchi (97% increase, $P = 0.013$; control, 39 ± 1.8%; *Foxg1cre*;*Srf*, 76 ± 2.5%; Fig. 2 *E*, *F*, and *J*). These data indicate that the establishment of the SM lineage is required to limit the number of cartilage cells in the trachea and main bronchi, but SM is required in only the main bronchi for the proper spatial restriction of cartilage cells.

Conditional Deletion of *Sox9* Resulted in a Loss of Cartilage and an Increase in SM in the Embryonic Upper Airways. To determine if cartilage is required for proper development of SM in the upper airways, we conditionally inactivated a critical cartilage differentiation gene, *Sox9*, in the lung by using a conditional allele of *Sox9* (*Sox9^{Fl}*) and *Foxg1-cre* (10, 11). *Foxg1-cre*;*Sox9 $^{Fl/Fl}$* (hereafter *Foxg1cre*;*Sox9*) embryos survived until E18.5, but died at birth of unknown causes. Alcian blue cartilage staining showed that there was a complete absence of cartilage in the *Foxg1cre*; *Sox9* trachea and main bronchi (Fig. 3 *A* and *B*). This result was confirmed by the lack of *Col2a1* expression at E14.5 (Fig. 3 *C* and *D*). With the exception of cartilage loss, *Foxg1cre*;*Sox9* mutant lungs appear grossly normal.

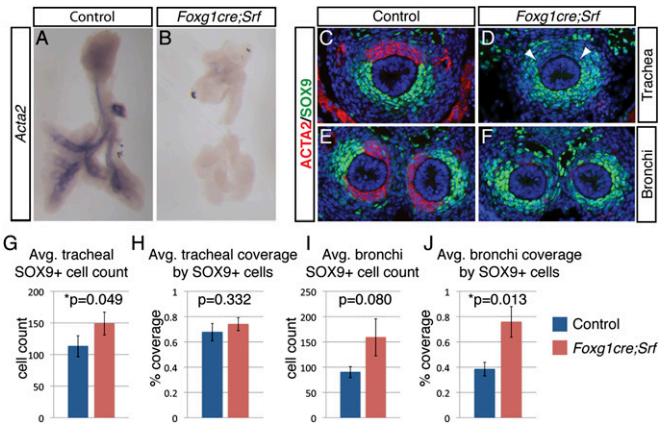

Fig. 2. Inactivation of *Srf* resulted in SM loss and cartilage increase in the upper airways. (*A* and *B*) *Acta2* RNA in situ hybridization in E12.5 lungs. (*C–F*) Immunostaining for ACTA2 (red), SOX9 (green), and nuclei (DAPI, blue) on transverse sections of E12.5 trachea or main bronchi. Arrowheads in *D* mark the limit of SOX9$^+$ airway coverage. (*G–J*) Graphs of control and *Foxg1cre*;*Srf* cell counts for SOX9$^+$ cells in the trachea (*G*) and main bronchi (*I*), and the percentage of the airway epithelium circumference covered by SOX9$^+$ cells in the trachea (*H*) and main bronchi (*J*). All graphs were made by using three independent mutant and control data points and averages are shown with SEM. *P* values are indicated.

To determine if this lack of cartilage affects the development of the SM, the number of ACTA2$^+$ cells and the percentage of the airway epithelium circumference in contact with ACTA2$^+$ cells (termed SM airway coverage) was assessed by using the same methods applied to the *Foxg1cre*;*Srf* mutants ($n = 3$ samples for each of mutant and control, and $n = 3$ sections per sample). In the trachea, trending toward significance, an increase in ACTA2$^+$ cells was observed in the mutant compared with control (49% increase, $P = 0.090$; control, 38.4 ± 1.3; *Foxg1cre*;*Sox9*, 57.2 ± 7.3; Fig. 3 *E*, *F*, and *I*). No difference was observed in the tracheal SM airway coverage ($P = 0.644$; control, 38 ± 5.5%; *Foxg1cre*;*Sox*9, 36 ± 2.8%; Fig. 3 *E*, *F*, and *J*). In the main bronchi, there was a significant increase in ACTA2$^+$ cells (97% increase, $P = 0.026$; control, 76.7 ± 6.8; *Foxg1cre*;*Sox9*, 151 ± 18.7), and there was a significant increase in SM airway coverage (72% increase, $P = 0.002$; control, 55 ± 1.8%; *Foxg1cre*;*Sox9*, 95 ± 0.55%; Fig. 3 *G*, *H*, *K*, and *L*). These data indicate that the establishment of the cartilage lineage is required to limit the number of SM cells in the trachea and main bronchi, but cartilage is required in only the main bronchi for the proper spatial restriction of SM cells.

Conditional Deletion of *Sox9* Resulted in a Decreased Number and Density of Basal Cells in the Trachea. *Foxg1cre*;*Sox9* mutants survive past the stage of airway epithelial cell differentiation, allowing us to address if cartilage loss affects epithelial cell differentiation. To assess the effect on basal cells, we started with P63 as a marker for all airway basal cells (28). In the control trachea at E17.5, we observed that total basal cell density, calculated as the ratio of P63$^+$ cells to total luminal epithelium (i.e., E-cadherin, ECAD$^+$) cells, was greater ($P = 2.8 \times 10^{-6}$) on the ventral subcartilage portion of the trachea (56 ± 5.3%) than it was on the dorsal sub-SM portion (37 ± 6.7%; Fig. 4 *A*, *A′*, *A″*, *C*, *C′*, *C″*, and *H*). To determine if cartilage is required to establish this difference, we assessed basal cell number and density in *Foxg1cre*;*Sox9* mutant tracheas. We used the P63$^+$:ECAD$^+$ cell ratio to correct for any potential differences in trachea size. To assess for possible variations resulting from height, we analyzed sections from the high (anterior), middle, and low (posterior) trachea, then these were compiled into an overall average value. Although we observed a slight decrease in basal cell density from high to low sections within a sample, the same mutant–control relationship was observed at each individual height: the P63$^+$:ECAD$^+$ cell ratio was decreased in *Foxg1cre*;*Sox9* mutants compared with controls (Fig. 4 *C*, *D*, and *G*). An average across all heights showed a significant 41% decrease in basal cell density in cartilage deficient tracheas ($P = 0.013$; control, 52 ± 5.0%; *Foxg1cre*;*Sox9*, 33 ± 5.2%). We also observed that the basal cell density in *Foxg1cre*;*Sox9* tracheas (33 ± 5.2%) was comparable to the density of basal cells on the SM side in the control (37 ± 6.7%), both of which were much lower than the overall density of basal cells on the cartilage side in the control (56 ± 5.3%; Fig. 4 *A*, *B*, and *H*).

A subset of P63$^+$ basal cells also expresses KRT14. In the adult airway, these KRT14$^+$ cells have been shown to have high proliferative and repair potential in naphthalene-injured airways (21). Additionally, KRT14 overexpression has been shown to drive squamous cell metaplasia and precancerous lesion formation in the mouse lung (29). Surprisingly, in E17.5 control tracheas, we found KRT14$^+$ cells only on the cartilage side, suggesting that the SM or cartilage may play a role in establishing this bias (Fig. 4*E*). Consistent with this notion, fewer KRT14$^+$ cells were observed in *Foxg1cre*;*Sox9* tracheas compared with control (Fig. 4 *E* and *F*). These data suggest that cartilage plays a role in promoting tracheal basal cell development.

To elucidate the possible role of signaling molecules in this cartilage to epithelium communication, we performed quantitative real-time PCR (qRT-PCR) for key signaling pathway readouts by using control and *Foxg1cre*;*Sox9* mutant tracheas at E17.5. We assayed for expression of *Axin2*, *Id2*, and sprouty homolog 2 (*Spry2*), readouts of canonical WNT, BMP, and FGF signaling, respectively. We observed a significant decrease in *Spry2* expression (Fig. S1) but did not observe a consistent change in *Axin2* or *Id2* expression. The decrease in *Spry2* expression raised the possibility that reduced FGF signaling in *Foxg1cre*;*Sox9* tracheas may contribute to the effect of cartilage loss on basal cell density.

Conditional Deletion of *Sox9* Resulted in Precocious and Increased Club Cell Marker Expression but Did Not Affect Differentiated Cell Number at Birth. To determine if the observed decrease in basal cell number in the *Foxg1*;*Sox9* mutant is accompanied by an

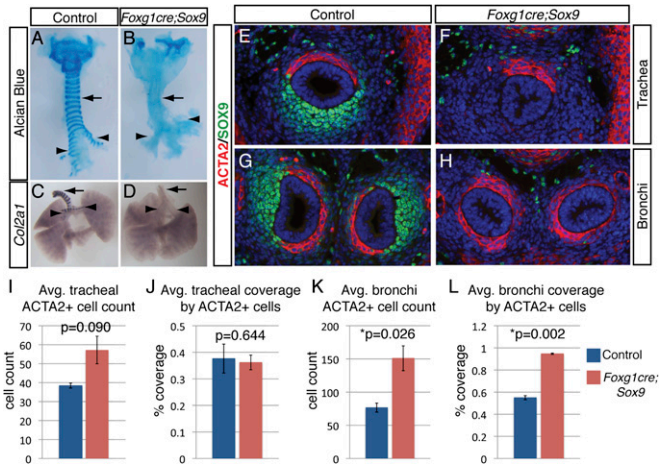

Fig. 3. Inactivation of *Sox9* resulted in cartilage loss and SM increase in the upper airways. (*A* and *B*) Alcian blue staining of E17.5 tracheas. (*C* and *D*) *Col2a1* RNA in situ hybridization of E14.5 lungs. Arrows indicate the trachea, and arrowheads indicate the main bronchi. (*E–H*) Immunostaining for ACTA2 (red), SOX9 (green), and nuclei (DAPI, blue) of transverse sections of E12.5 trachea or main bronchi. (*I–L*) Graphs of control and *Foxg1cre*;*Sox9* cell counts for ACTA2$^+$ cells in the trachea (*I*) and main bronchi (*K*) and the percentage of the airway epithelium circumference covered by ACTA2$^+$ cells in the trachea (*J*) and main bronchi (*L*). All graphs were made by using three independent mutant and control data points, and averages are shown with SEM. *P* values are indicated.

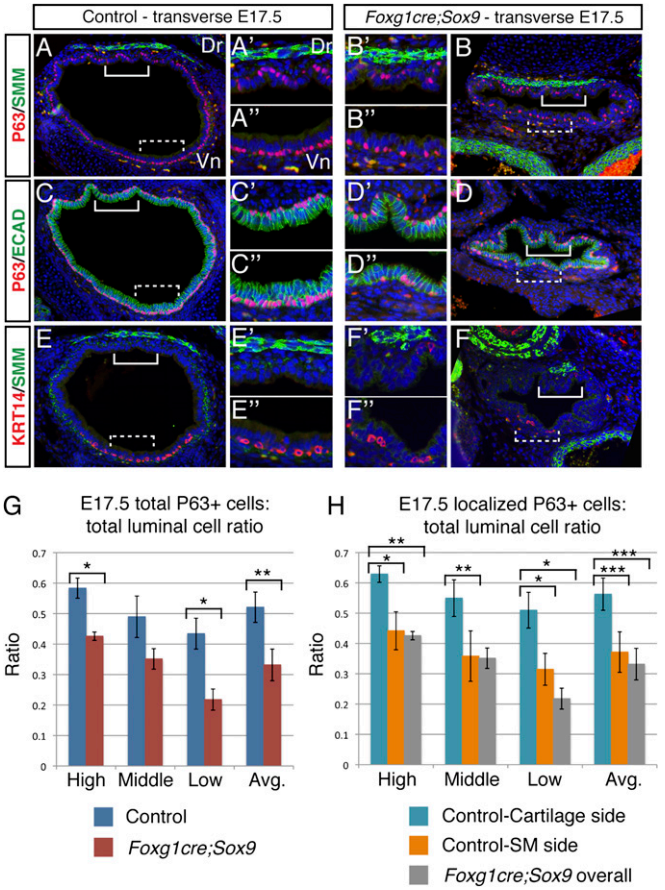

Fig. 4. Inactivation of *Sox9* resulted in decreased tracheal basal cell density. (*A*–*F*) Immunostaining for markers as indicated on E17.5 trachea transverse sections. Sections at middle height trachea level are shown as representative examples. Solid brackets indicate dorsal regions magnified in *A′*–*F′*. Dashed brackets indicate ventral regions magnified in *A′′*–*F′′*. (*G*) Basal cell density (ratio of P63$^+$ cells to total luminal cells) was compared between control and *Foxg1cre*;*Sox9* tracheas at high, middle, and low heights as well as an overall average (Avg.) across the trachea. (*H*) In control tissue, basal cell density on the cartilage side and SM side were compared with the overall basal cell density in *Foxg1cre*;*Sox9* tracheas across high, middle, and low heights as well as an overall average (Avg.). For each level, graphs were made by using four independent mutant and control data points. For the overall average, all 12 independent high, middle, and low data points were averaged. All graphs are shown with SEM (*$P < 0.05$, **$P < 0.01$, and ***$P < 0.001$). Dr, dorsal; Vn, ventral.

alteration in differentiated airway cell number, we assessed club, ciliated, and goblet cell numbers in the mutant and control tracheas across the three heights. Similar to our analysis of basal cells, we used a differentiated cell to ECAD$^+$ epithelial cell ratio to correct for any potential differences in trachea size. In the control at E18.5 just before birth, we found that club cell density was greater on the dorsal side of the trachea whereas ciliated cell density was greater on the ventral side of the trachea, raising the possibility that the surrounding mesenchymal cells may contribute to this bias (Fig. 5*A*). However, when comparing E18.5 *Foxg1cre*;*Sox9* mutants to control across all tracheal heights, we did not observe any statistically significant differences in the density of SCGB1A1$^+$ club cells or TUBA1A$^+$ (also known as α-Tubulin) ciliated cells (Fig. 5 *A*, *B*, *E*, and *F*). Goblet cells were rarely found in control or mutant tracheas and the *Muc5ac* transcript level, as determined by qRT-PCR, was low in both genotypes. Despite the lack of difference in SCGB1A1$^+$ cell density between mutant and control, the SCGB1A1 staining in *Foxg1cre*;*Sox9* tracheas consistently appeared more intense than in the control tissue. To determine if this intensity difference reflected a higher *Scgb1a1* transcript level, we performed qRT-PCR. We found that *Scgb1a1* was expressed at a fourfold higher level in *Foxg1cre*; *Sox9* tracheas than in control (Fig. 5*G*). This suggests that, although loss of cartilage does not affect total club cell number, it may impact the differentiation state of club cells. To address if there is a defect in the timing of differentiation, we examined SCGB1A1 expression at earlier stages. At E17.0, there were few dim SCGB1A1$^+$ club cells detected in the control. However, more intensely stained SCGB1A1$^+$ cells were consistently observed in the mutant (Fig. 5 *C* and *D*), suggesting precocious differentiation.

Discussion

In the present study, we used a genetic approach that revealed clear in vivo evidence for tissue dependence and possible cross-talk in the development of upper airway SM and cartilage. Temporal assessment of normal upper airways revealed that SM and cartilage emerge simultaneously in complementary spatial patterns. Loss of SM or cartilage resulted in an increase in cell number (in the trachea and bronchi) and spatial domain (in the bronchi) of the remaining tissue lineage. Our results thereby indicate that the juxtaposition of these tissues is established primarily through a communication, either direct or indirect, between SM and cartilage. Additionally, in the absence of cartilage, basal cell density was decreased and club cells developed precociously. These findings define the nature and extent of the feedback among tissues in the developing mouse upper airways.

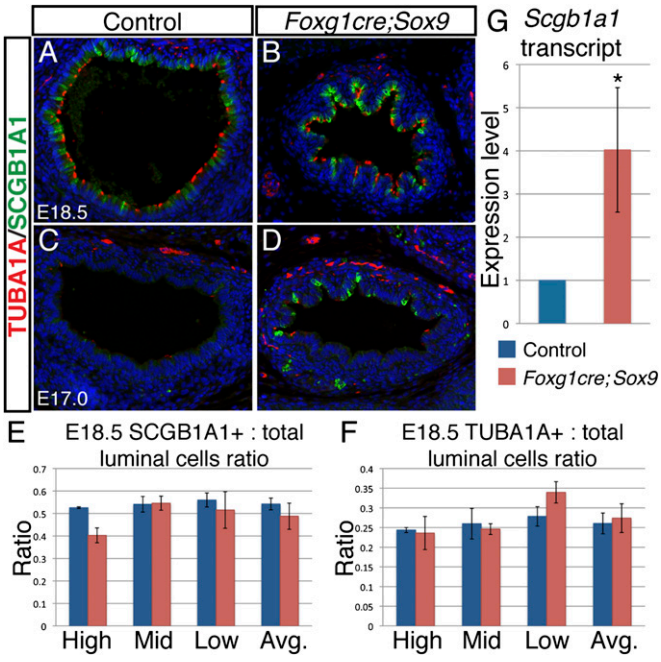

Fig. 5. Inactivation of *Sox9* did not affect differentiated cell number but did lead to increased club cell gene expression. (*A*–*D*) Immunostaining for TUBA1A (red), SCGB1A1 (green), and nuclei (DAPI, blue) on middle height transverse sections of tracheas at indicated stages. Red signal in the mesenchyme is not specific to ciliated cells. (*E* and *F*) Quantification of SCGB1A1$^+$ cells (*E*) and TUBA1A$^+$ cells (*F*) as a percentage of total luminal epithelial cells at high, middle, and low tracheal heights, and an overall average (Avg.). For each level, graphs were made by using four independent mutant and control data points. For the overall average, all 12 independent high, middle, and low data points were averaged. All cell count graphs are shown with SEM. No statistically significant differences were observed between mutant and control. (*G*) qRT-PCR of *Scgb1a1* expression in E18.5 *Foxg1cre*;*Sox9* tracheas compared with controls, shown with SD (*$P = 0.02$).

When two tissues form in spatial complementation within the same temporal window, their coordinated development could result from a precise allocation of upstream determinants, or from a continuous communication between the tissues as they develop. In the first scenario, the patterning of each individual tissue would be independent of the adjacent tissue. In the second scenario, the patterning of each individual tissue would be influenced by the development of the adjacent tissue. Our data from conditional mutants suggest that proper upper airway mesenchyme patterning primarily results from the second scenario and the impacts are reciprocal, i.e., SM loss had similar effects on cartilage patterning as loss of cartilage did on SM patterning (Fig. 6). Furthermore, our results highlight a potential difference in the relationship of these tissues in the trachea versus the bronchi. In the trachea, a loss of SM or cartilage led to an increase in cell number, but not a change in spatial domain of the remaining tissue type. In the main bronchi, loss of SM or cartilage led to an increase in cell number and an increase in the spatial domain of the remaining tissue type. Our analyses determined that the development of these tissue lineages in the control, as well as loss of these lineages in the mutants, occurs during comparable time windows in the trachea and bronchi. Thus, the difference in phenotype in the trachea and bronchi likely reflects a true disparity in cellular properties, rather than a difference in the developmental timing of these lineages in the trachea versus bronchi. Taken together, our findings suggest that, in the upper airways, SM and cartilage develop codependently, with the exception of airway coverage in the trachea (Fig. 6).

It remains to be determined whether the increase in cell number in the remaining lineage arises from increased cell proliferation or cell fate change. An increase in cell proliferation would suggest that one lineage limits the proliferation of the adjacent lineage. A change in cell fate would suggest that there is plasticity in differentiation potential, and cells normally allocated to one tissue lineage could switch to the other lineage in the absence of appropriate differentiation factors, e.g., *Srf* or *Sox9*. The latter situation is plausible, as airway SM and cartilage are thought to both originate from splanchnic mesoderm. Preliminary genetic lineage tracing from our laboratory has shown that, in normal upper airways, a few *Sox9-cre*–labeled cartilage lineage cells and a few *Transgelin-cre* (also known as *Sm22-cre*) labeled SM lineage cells can take on SM or cartilage fate, respectively. These results suggest that there is a small degree of plasticity in cell fate in normal upper airway development. Whether this mechanism underlies the cell number increase seen in *Foxg1cre*;*Srf* and *Foxg1cre*;*Sox9* airways remains to be determined; it awaits additional genetic tools to allow for lineage tracing within mutants. At the molecular level, the inhibitory action that one lineage exerts on the other could be mediated directly through secreted signals and/or cell surface molecules. Additionally, ECM composition and/or tensile forces may provide indirect communication for proper tissue patterning. When one lineage, either SM or cartilage, fails to differentiate, the cells that remain in that lineage's domain may exert a distinct physical resistance on the surrounding tissues, which may influence the migratory and/or proliferative behavior of the juxtaposed cell type.

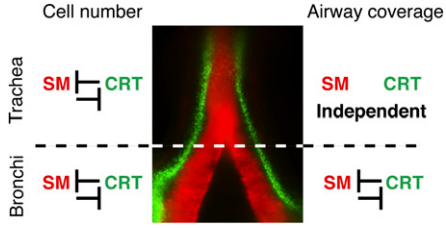

Fig. 6. A model summarizing distinct relationships between SM and cartilage in the developing upper airways. (*Center*) Whole-mount WT E12.5 upper airway stained with ACTA2 (red) and SOX9 (green). Codependent relationship between SM and cartilage (*Left*) with regard to cell number in the trachea (*Upper*) and bronchi (*Lower*) and airway coverage (*Right*) in the bronchi (*Lower*), and (*Upper*) independent relationship between SM and cartilage with regard to airway coverage in the trachea.

Previous experiments have shown that coculture of tracheal mesenchyme with distal lung epithelium can change the fate of the epithelial cells from distal to proximal (24). Although these experiments did not distinguish between dorsal vs. ventral mesenchyme, they demonstrated the instructive capacity of the tracheal mesenchyme. In normal E17.0 to E18.5 tracheas, we observed that basal and ciliated cell density is greater in the epithelium underlying cartilage (ventral) than in the epithelium underlying SM (dorsal), whereas the club cell density exhibits the opposite bias. It is important to note that in the adult trachea, $P63^+$ basal cells, $TUBA1A^+$ ciliated cells, and $SCGB1A1^+$ club cells become evenly distributed throughout the epithelium (Fig. S2 *A* and *B*). Despite the transient nature of this epithelial asymmetry, it would be interesting to examine if a bias reemerges during repair after injury, as common developmental mechanisms are often redeployed during regenerative processes (30). Results from our cartilage-deficient mutants support the possibility that cartilage may serve as a developmental niche for basal cells. However, cartilage is not required for the promotion of ciliated cells. The earlier emergence of club cells as well as an increase in club cell marker expression in the cartilage-deficient mutants suggest that cartilage may have inhibitory effects on club cell differentiation, although not to the extent of affecting the final club cell number. It should be noted that in the absence of the cartilage, the upper airways are often deformed, raising the possibility that a change in airway biomechanics may contribute to the observed shifts in epithelial cell composition. Regardless of the mechanism, our findings demonstrate that precise airway mesenchyme patterning is essential for the proper allocation of epithelial cells during development. A previous study demonstrated that in adult airways postinjury, SM cells up-regulate *Fgf10* expression, which in turn activates variant club cells and promotes epithelial repair (30). These findings are in line with the implications of our results, and together these suggest that airway SM and cartilage may serve as active microenvironments for the epithelium in the developing and adult lung.

One possible explanation for the early mesenchymal and late epithelial phenotypes seen in *Foxg1cre*;*Sox9* mutants is that loss of *Sox9* in the proximal mesenchyme resulted in a distalization of the upper airways. Distalization would be consistent with the observed SM expansion phenotype, as the normal intrapulmonary airways located more distal to the main bronchi are surrounded by SM. Distalization would also be consistent with the observed basal cell decrease, as basal cell density decreases along the proximal to distal axis of the upper airways. To determine if distalization is a plausible mechanism, we assessed expression of the proximal epithelial marker SOX2 and the distal epithelial marker NKX2.1 (Fig. S3). We observed no difference in the proximal/distal marker expression pattern, suggesting that upper airway distalization is likely not responsible for the observed phenotypes in *Foxg1cre*;*Sox9* mutants.

Our study provides insight on the causal relationships among the complex pathologic conditions observed in patients with upper airway disorders. For example, it is generally believed that patients with tracheomalacia and bronchomalacia experience airway collapse because of reduced or disorganized cartilage. However, patient airways may also exhibit an expansion of SM, which would contribute to airway constriction. Recent data from cystic fibrosis mouse and pig models revealed that before any reported epithelial defects, these models exhibit deformed tracheal cartilage, misoriented SM, and increased SM gene expression (31–33). Our findings support the possibility that, in prominent airway diseases such as cystic fibrosis, the disorganized mesenchymal structures may contribute to the epithelial defects central to the pathophysiology of the disease.

Materials and Methods

Mice. Embryos were dissected from time-mated mice, counting 12 noon on the day when the vaginal plug was found as E0.5. *Srf*^{Fl}, *Sox9*^{Fl}, and *Foxg1-cre* alleles have been previously described (11, 27, 34). Mutants were obtained by crossing a female that was homozygous for the conditional allele, to a male that was heterozygous for both *cre* and the conditional allele. Non-*cre* littermate embryos were used as controls. All mouse protocols were approved by the Animal Care and Use Committee of the University of Wisconsin–Madison.

Whole-Mount in Situ Hybridization. Lungs were dissected in phosphate buffered saline (PBS), fixed in 4% paraformaldehyde overnight at 4 °C, and then dehydrated to 100% MeOH. Whole-mount in situ hybridization was carried out by using established protocols (35).

Immunofluorescence Staining. Embryos were dissected in 1% PBS solution, fixed in 4% paraformaldehyde overnight at 4 °C, processed for paraffin embedding, and sectioned at 5μm. Immunofluorescence was carried out by using standard protocols and citric acid antigen retrieval. The antibodies used are listed in *SI Materials and Methods*.

Cartilage Staining. Tracheas were dissected in PBS solution and fixed in 95% EtOH. Alcian blue staining was carried out according to standard protocols.

Cell Quantification and Statistical Analysis. Immunofluorescently labeled cells were manually counted. For each experiment at E12.5, 3 separate mutant–control littermate pairs were analyzed. For each mutant or control sample, three sections were quantified, and the numbers were averaged to represent the sample. For each experiment at E17.5 or E18.5, four sets of mutant–control pairs were analyzed. For each mutant or control sample, three sections representing high, middle, or low heights were quantified. Mutant and controls were compared within high, middle, or low groups, or across all height groups for the "average" comparison. A paired Student *t* test was used to determine significance, and SEM was calculated.

Quantitative Real-Time PCR. Tracheas for qRT-PCR were dissected in PBS and homogenized using the TissueLyser (Qiagen) in TRIzol and then stored at −80 °C. The reverse transcription reaction was done by using the SuperScript III First Stand kit (Invitrogen). qRT-PCR was carried out by using Power SYBR green (Applied Biosystems) and standard protocols. Primer sets used are listed in *SI Materials and Methods*.

ACKNOWLEDGMENTS. We thank members of the laboratory of X.S. for helpful discussions, Amber Lashua for expert technical assistance, and Tom Havighurst (University of Wisconsin Carbone Cancer Center Biostatistics Consulting Clinic) for guidance on statistical analysis. This work was supported by National Science Foundation Graduate Research Fellowship 2011101268 (to E.A.H.), National Heart, Lung, and Blood Institute Grant HL113870, March of Dimes Grant 6-FY10-339 (to X.S.), and Cystic Fibrosis Foundation Grant SUN1210 (to X.S.).

1. Cardoso WV, Whitsett JA (2008) Resident cellular components of the lung: Developmental aspects. *Proc Am Thorac Soc* 5(7):767–771.
2. Morrisey EE, Hogan BL (2010) Preparing for the first breath: Genetic and cellular mechanisms in lung development. *Dev Cell* 18(1):8–23.
3. Austin J, Ali T (2003) Tracheomalacia and bronchomalacia in children: Pathophysiology, assessment, treatment and anaesthesia management. *Paediatr Anaesth* 13(1):3–11.
4. Doshi J, Krawiec ME (2007) Clinical manifestations of airway malacia in young children. *J Allergy Clin Immunol* 120(6):1276–1278.
5. Mailleux AA, et al. (2005) Fgf10 expression identifies parabronchial smooth muscle cell progenitors and is required for their entry into the smooth muscle cell lineage. *Development* 132(9):2157–2166.
6. Peng T, et al. (2013) Coordination of heart and lung co-development by a multipotent cardiopulmonary progenitor. *Nature* 500(7464):589–592.
7. Yoshida T, et al. (2003) Myocardin is a key regulator of CArG-dependent transcription of multiple smooth muscle marker genes. *Circ Res* 92(8):856–864.
8. Goss AM, et al. (2011) Wnt2 signaling is necessary and sufficient to activate the airway smooth muscle program in the lung by regulating myocardin/Mrtf-B and Fgf10 expression. *Dev Biol* 356(2):541–552.
9. Miller LA, et al. (2004) Role of Sonic hedgehog in patterning of tracheal-bronchial cartilage and the peripheral lung. *Dev Dyn* 231(1):57–71.
10. Bi W, Deng JM, Zhang Z, Behringer RR, de Crombrugghe B (1999) Sox9 is required for cartilage formation. *Nat Genet* 22(1):85–89.
11. Akiyama H, Chaboissier MC, Martin JF, Schedl A, de Crombrugghe B (2002) The transcription factor Sox9 has essential roles in successive steps of the chondrocyte differentiation pathway and is required for expression of Sox5 and Sox6. *Genes Dev* 16(21):2813–2828.
12. Lefebvre V, Li P, de Crombrugghe B (1998) A new long form of Sox5 (L-Sox5), Sox6 and Sox9 are coexpressed in chondrogenesis and cooperatively activate the type II collagen gene. *EMBO J* 17(19):5718–5733.
13. Bell SM, et al. (2008) R-spondin 2 is required for normal laryngeal-tracheal, lung and limb morphogenesis. *Development* 135(6):1049–1058.
14. Vermot J, Niederreither K, Garnier JM, Chambon P, Dollé P (2003) Decreased embryonic retinoic acid synthesis results in a DiGeorge syndrome phenotype in newborn mice. *Proc Natl Acad Sci USA* 100(4):1763–1768.
15. Li M, et al. (2008) Mesodermal deletion of transforming growth factor-beta receptor II disrupts lung epithelial morphogenesis: cross-talk between TGF-beta and Sonic hedgehog pathways. *J Biol Chem* 283(52):36257–36264.
16. Tiozzo C, et al. (2009) Fibroblast growth factor 10 plays a causative role in the tracheal cartilage defects in a mouse model of Apert syndrome. *Pediatr Res* 66(4):386–390.
17. Rackley CR, Stripp BR (2012) Building and maintaining the epithelium of the lung. *J Clin Invest* 122(8):2724–2730.
18. Zariwala MA, Knowles MR, Omran H (2007) Genetic defects in ciliary structure and function. *Annu Rev Physiol* 69:423–450.
19. Boucherat O, Boczkowski J, Jeannotte L, Delacourt C (2013) Cellular and molecular mechanisms of goblet cell metaplasia in the respiratory airways. *Exp Lung Res* 39(4-5):207–216.
20. Daniely Y, et al. (2004) Critical role of p63 in the development of a normal esophageal and tracheobronchial epithelium. *Am J Physiol Cell Physiol* 287(1):C171–C181.
21. Hong KU, Reynolds SD, Watkins S, Fuchs E, Stripp BR (2004) Basal cells are a multipotent progenitor capable of renewing the bronchial epithelium. *Am J Pathol* 164(2):577–588.
22. Hong KU, Reynolds SD, Watkins S, Fuchs E, Stripp BR (2004) In vivo differentiation potential of tracheal basal cells: Evidence for multipotent and unipotent subpopulations. *Am J Physiol Lung Cell Mol Physiol* 286(4):L643–L649.
23. Rock JR, et al. (2009) Basal cells as stem cells of the mouse trachea and human airway epithelium. *Proc Natl Acad Sci USA* 106(31):12771–12775.
24. Shannon JM, Nielsen LD, Gebb SA, Randell SH (1998) Mesenchyme specifies epithelial differentiation in reciprocal recombinants of embryonic lung and trachea. *Dev Dyn* 212(4):482–494.
25. Borthwick DW, Shahbazian M, Krantz QT, Dorin JR, Randell SH (2001) Evidence for stem-cell niches in the tracheal epithelium. *Am J Respir Cell Mol Biol* 24(6):662–670.
26. Li Y, Gordon J, Manley NR, Litingtung Y, Chiang C (2008) Bmp4 is required for tracheal formation: A novel mouse model for tracheal agenesis. *Dev Biol* 322(1):145–155.
27. Miano JM, et al. (2004) Restricted inactivation of serum response factor to the cardiovascular system. *Proc Natl Acad Sci USA* 101(49):17132–17137.
28. Rock JR, Hogan BL (2011) Epithelial progenitor cells in lung development, maintenance, repair, and disease. *Annu Rev Cell Dev Biol* 27:493–512.
29. Dakir ELH, Feigenbaum L, Linnoila RI (2008) Constitutive expression of human keratin 14 gene in mouse lung induces premalignant lesions and squamous differentiation. *Carcinogenesis* 29(12):2377–2384.
30. Volckaert T, et al. (2011) Parabronchial smooth muscle constitutes an airway epithelial stem cell niche in the mouse lung after injury. *J Clin Invest* 121(11):4409–4419.
31. Bonvin E, et al. (2008) Congenital tracheal malformation in cystic fibrosis transmembrane conductance regulator-deficient mice. *J Physiol* 586(13):3231–3243.
32. Meyerholz DK, et al. (2010) Loss of cystic fibrosis transmembrane conductance regulator function produces abnormalities in tracheal development in neonatal pigs and young children. *Am J Respir Crit Care Med* 182(10):1251–1261.
33. Pan J, Luk C, Kent G, Cutz E, Yeger H (2006) Pulmonary neuroendocrine cells, airway innervation, and smooth muscle are altered in Cftr null mice. *Am J Respir Cell Mol Biol* 35(3):320–326.
34. Hébert JM, McConnell SK (2000) Targeting of cre to the Foxg1 (BF-1) locus mediates loxP recombination in the telencephalon and other developing head structures. *Dev Biol* 222(2):296–306.
35. Abler LL, et al. (2011) A high throughput in situ hybridization method to characterize mRNA expression patterns in the fetal mouse lower urogenital tract. *J Vis Exp* 54:2912.